AD-A042 429 CONSTRUCTION ENGINEERING RESEARCH LAB (ARMY) CHAMPAI--ETC F/G 18/6
THE EFFECTS OF FAST AND THERMAL NEUTRON FLUX AND GAMMA RADIATIO--ETC(U)
JUL 77 D C SIEBER, R G MCCORMACK

UNCLASSIFIED CERL-TR-E-112 NL

| OF |
AD
A042429

END
DATE
FILMED
8-77
DDC

construction
engineering
research
laboratory

INTERIM REPORT E-112
July 1977

THE EFFECTS OF FAST AND THERMAL NEUTRON FLUX AND GAMMA RADIATION ON THE TRANSMISSION CHARACTERISTICS OF OPTICAL FIBERS

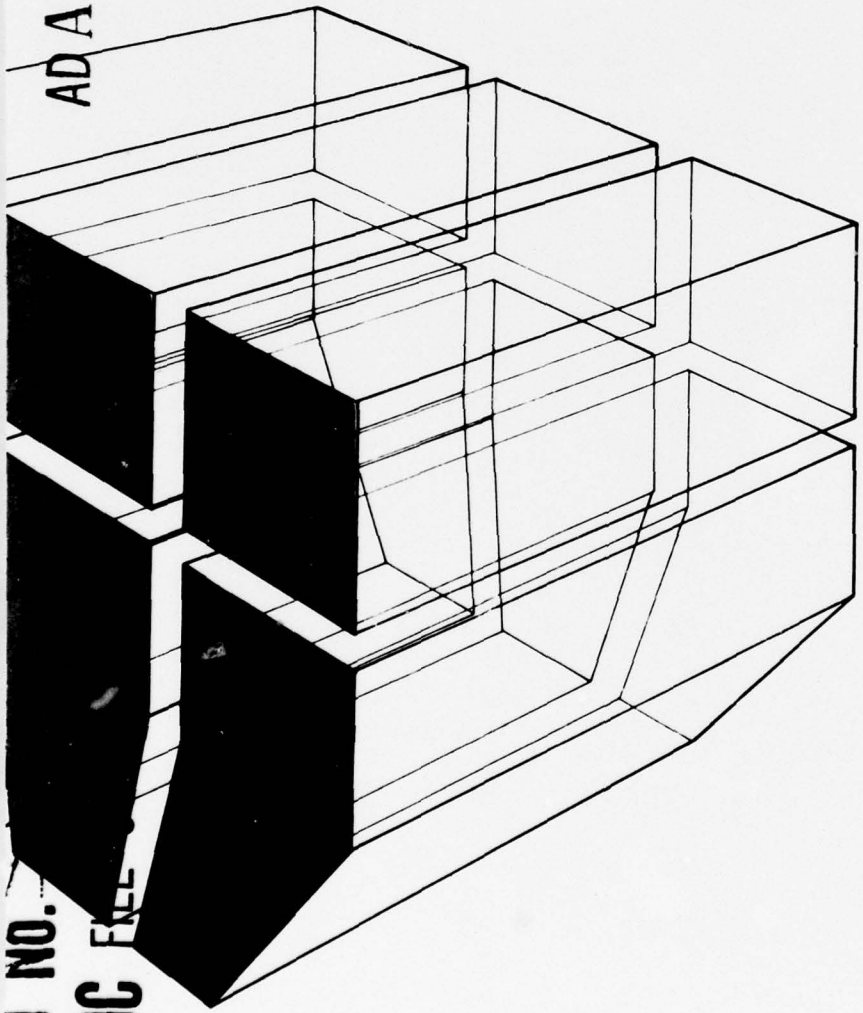

by
D. C. Sieber
R. G. McCormack
W. J. Croisant

SECURITY CLASSIFICATION OF THIS PAGE *(When Data Entered)*

REPORT DOCUMENTATION PAGE

READ INSTRUCTIONS BEFORE COMPLETING FORM

1. REPORT NUMBER: CERL-IR-E-112	2. GOVT ACCESSION NO.
3. RECIPIENT'S CATALOG NUMBER	
4. TITLE *(and Subtitle)*: THE EFFECTS OF FAST AND THERMAL NEUTRON FLUX AND GAMMA RADIATION ON THE TRANSMISSION CHARACTERISTICS OF OPTICAL FIBERS.	5. TYPE OF REPORT & PERIOD COVERED: INTERIM report
	6. PERFORMING ORG. REPORT NUMBER
7. AUTHOR(s): D. C. Sieber, R. G. McCormack, W. J. Croisant	8. CONTRACT OR GRANT NUMBER(s)
9. PERFORMING ORGANIZATION NAME AND ADDRESS: CONSTRUCTION ENGINEERING RESEARCH LABORATORY, P.O. Box 4005, Champaign, IL 61820	10. PROGRAM ELEMENT, PROJECT, TASK AREA & WORK UNIT NUMBERS: 4A762719AT40-A1-022
11. CONTROLLING OFFICE NAME AND ADDRESS	12. REPORT DATE: July 1977
	13. NUMBER OF PAGES: 26
14. MONITORING AGENCY NAME & ADDRESS *(if different from Controlling Office)*	15. SECURITY CLASS. *(of this report)*: Unclassified
	15a. DECLASSIFICATION/DOWNGRADING SCHEDULE

16. DISTRIBUTION STATEMENT *(of this Report)*

Approved for public release; distribution unlimited.

17. DISTRIBUTION STATEMENT *(of the abstract entered in Block 20, if different from Report)*

18. SUPPLEMENTARY NOTES

Copies are obtainable from National Technical Information Service
Springfield, VA 22151

19. KEY WORDS *(Continue on reverse side if necessary and identify by block number)*

optical fibers
fast and thermal neutron flux
gamma radiation

20. ABSTRACT *(Continue on reverse side if necessary and identify by block number)*

This report presents the results of a study of the effects of nuclear radiation on the light transmission characteristics of optical fibers. Two types of radiation were used: 1800-MW pulses of primarily thermal neutrons (10^{12} n/cm^2), and a 20-minute exposure of thermal and fast neutrons and gamma radiation. Three representative types of optical fibers were tested: low-loss fused silica, medium-loss lead silicate with borosilicate cladding, and plastic.

Next page

10 to the 12th power n/sq cm.

DD FORM 1 JAN 73 1473 EDITION OF 1 NOV 65 IS OBSOLETE

UNCLASSIFIED

SECURITY CLASSIFICATION OF THIS PAGE *(When Data Entered)*

405279

Block 20 continued.

The fibers' radiation-induced attenuation changes and luminescence were monitored. Thermal neutrons were found to induce both attenuation increases and luminescence in all three fiber types. Fibers made of lead silicate with borosilicate cladding were found to develop a permanent attenuation increase of greater than 300 dB/km, making the fiber useless for most communication systems.

FOREWORD

This research was conducted for the Directorate of Military Construction, Office of the Chief of Engineers (OCE) under Project 4A762719AT40, "Mobility, Soils, and Weapons Effects"; Technical Area A1, "Weapons Effects and Protective Structures"; Work Unit 022, "EMI Circumvention by Fiber Optic Transmission." The applicable QCR is 1.03.010. The OCE Technical Monitor was Mr. H. McCauley, DAEN-MCE-D.

The study was conducted by the Electrical-Mechanical Branch (EPM), Energy and Power Division (EP), U. S. Army Construction Engineering Research Laboratory (CERL), Champaign, IL. The CERL Principal Investigator was Mr. R. G. McCormack.

Appreciation is expressed to Dr. J. Verdeyen of the University of Illinois at Urbana-Champaign for his assistance and to Mr. Martin Santic of CERL for planning the experiment.

Mr. R. G. Donaghy is Chief of EP and Mr. M. J. Pollock is Chief of EPM. COL J. E. Hays is Commander and Director of CERL and Dr. L. R. Shaffer is Technical Director.

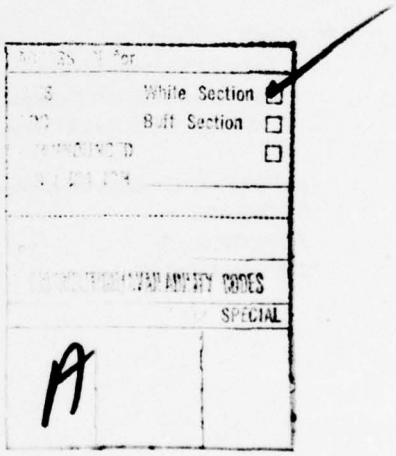

CONTENTS

FIGURES

THE EFFECTS OF FAST AND THERMAL NEUTRON FLUX AND GAMMA RADIATION ON THE TRANSMISSION CHARACTERISTICS OF OPTICAL FIBERS

1 INTRODUCTION

Background

A fiber optic link consists of a light source whose intensity is modulated by a transmitter, an optical fiber to transmit the light, and a photodetector. The photodetector, which is sensitive to the optical signal transmitted by the fiber, produces an electrical signal which is proportional to the output of the modulated light source. Research over the past several years[1] has indicated that replacing conventional electrical cable used in data transmission with fiber optic links has several advantages:

1. Reduced susceptibility to electromagnetic interference (EMI) resulting from electromagnetic fields and pulses (EMF and EMP). Electromagnetic interference is a major problem in the design of nuclear EMP-hardened facilities. While conventional electrical cables are very susceptible to EMP and EMF, tests conducted at the U. S. Army Construction Engineering Research Laboratory (CERL)[2] have determined that high intensity EMP and EMI environments have no appreciable effect on fiber optic links.

2. Electrical isolation. Because optical fibers are made of nonconductive glass or plastic, grounding problems between the transmitter and the receiver are not possible. Optical fibers also circumvent the problem of crosstalk between cables, because electrical current is not employed in transmission.

3. Wide bandwidth. With current optical fiber technology, fibers have a bandwidth capability of 100 GHz. This wide bandwidth permits simultaneous transmission of several thousand signals over a single fiber using multiplexing techniques. Bandwidth capability of this size is not possible in conventional metallic conductors.

4. Reduced size. Optical fiber links are also smaller and weigh less than conventional electrical cables.

Although these numerous advantages have caused increased use of optical fiber links in military systems, one possible problem with optical fiber links is that nuclear radiation is known to create coloration centers in optical material, thus causing an increase in the attenuation of the light transmitted through the material.[3] Radiation can also generate light within the optical material. Any nuclear-radiation-induced effect in the transmission characteristics of an optical fiber link may prove to be a limitation in a military communications system which is deployed in a potential nuclear environment.

Previous research on the effects of nuclear radiation has been limited to the effects of fast neutrons, high energy electrons, and gamma, X-ray, and alpha radiation.[4] This study primarily investigated the effects of thermal neutron radiation, which had not previously been studied.

Objective

The objective of this study was to augment past research on the effects of radiation on optical fibers by investigating the following specifi effects:

1. Possible short-term effects of thermal neutron flux on various commercially available optical fibers. The short-term effects to be investigated were attenuation variations and radiation-induced luminescence. (See the glossary for definition of attenuation and short- and long-term changes.)

2. Possible long-term attenuation changes in various commercially available fibers due to thermal neutron flux.

3. Possible long- and short-term effects on the transmittance of various fibers in an environment consisting of gamma radiation, fast neutron flux, and thermal neutron flux.

---

[1] R. L. Gallawa, *Optical Fiber Links for Telecommunication* (U. S. Army Strategic Communications Command, 1973).

[2] R. G. McCormack and D. C. Sieber, *Fiber Optic Communications Link Performance in EMP and Intense Light Transient Environments*, Interim Report E-94/ADA032126 (U. S. Army Construction Engineering Research Laboratory, 1976).

[3] R. D. Manual, E. J. Schiel, S. Kronenburg, and R. A. Lux, "Effect of Neutron- and Gamma Radiation on Glass Optical Waveguides," *Applied Optics* (September 1973); and J. A. Wall and J. F. Bryant, *Radiation Effects on Fiber Optics*, AFCRL-TR-75-0190 (Air Force Cambridge Research Laboratories, 1975).

[4] Manual et al; Wall and Bryant; and P. L. Mattern, L. M. Watkins, C. D. Skoog, J. R. Brandon, and E. H. Barsis, *The Effects of Radiation on the Absorption and Luminescence of Fiber Optic Waveguides and Materials* (Sandia Laboratories, 1974).

Approach

Three representative types of optical fibers were studied: (1) low-loss fused silica, (2) all-plastic, and (3) medium-loss lead-silicate with borosilicate cladding.

The study consisted of two experimental phases: (1) determination of the effects of thermal neutron flux on the transmission characteristics of an optical fiber, and (2) determination of the combined effects of fast neutron flux, thermal neutron flux, and gamma radiation.

Three effects may occur due to exposure to a thermal neutron environment: luminescence, short-term attenuation, and long-term attenuation. Because luminescence and short-term attenuation cannot be detected using a simple pre- and post-pulse measurement technique, they were monitored by measuring the transmission of the fibers during the thermal neutron pulse (10^{12} n/cm^2). The amplitude and time duration of any luminescence detected during the pulse were determined, as were the maximum value and time duration of short-term attenuation detected. Long-term attenuation due to the thermal neutron flux was detected by measuring the transmission of the fiber for several minutes after the thermal neutron pulse. The duration and amplitude of the long-term attenuation was determined from this measurement.

In the second phase of the study, the fiber was subjected to a 20-minute steady-state exposure to combined fast and thermal neutrons and gamma radiation. This radiation exposure could cause two effects: radiation-induced attenuation during the exposure, and a long-term attenuation effect after the exposure. To determine if there was any radiation-induced attenuation during the exposure, the transmission of the fiber was measured several times during exposure. Long-term attenuation was identified by measuring the fiber transmission several times after exposure.

Scope

This study was not intended to investigate the mechanism by which fast or thermal neutron flux interacts with optical fiber materials to affect the transmission characteristics. Consequently, no attempt was made to quantitatively determine the effects that expected threat-level nuclear environments would cause on any optical fiber link.

2 EXPERIMENTAL PROCEDURES

Test Samples

This section describes the three representative types of commercially available optical fibers tested in this study.

Plastic Fiber

Plastic fibers, which are inexpensive but have very high attenuation, consist of a polymethyl methacrylate or polystyrene core and a cladding of a polymer having an index of refraction less than the core. The fiber used in this study was plastic monofilament with a polystyrene core and an acrylic plastic cladding.

Low-Loss Fused Silica Fibers

Fused silica fibers, which are drawn from pure fused silica, have attenuations of less than 50 dB/km. The fiber used in this study consisted of a single optical fiber with a polyester elastomer jacket. The core material is pure fused silica and the cladding material is a high-quality optical plastic. The maximum attenuation of this fiber is 20 dB/km at a wavelength of 8200 Å.

Medium-Loss Borosilicate and Lead-Silicate Fibers

These fibers are drawn from standard optical glass. The fiber used in this study has a borosilicate cladding and a lead-silicate core. Its attenuation is 400 dB/km.

Experimental Setup

Figure 1 is a schematic of the basic experimental setup used in both phases of the study. The setup consisted of a laser light source, a light chopper, a focusing lens, 10-m length of optical fiber placed in a nuclear reactor port (thermal or beam), a photomultiplier, three oscilloscopes, and a digital recording oscilloscope. The three optical fibers along with each element of the experimental setup are described below:

Light Source

A 5-mW helium-neon laser (wavelength = 6328 Å) was used as the light source because its highly collimated beam enables simplified coupling into the fiber.

Light Chopper

The light beam was chopped by a mechanical chopper. The chopped light level was used rather than a constant light level so that the light amplitude measurement would not be susceptible to any dc level change in the measurement equipment.

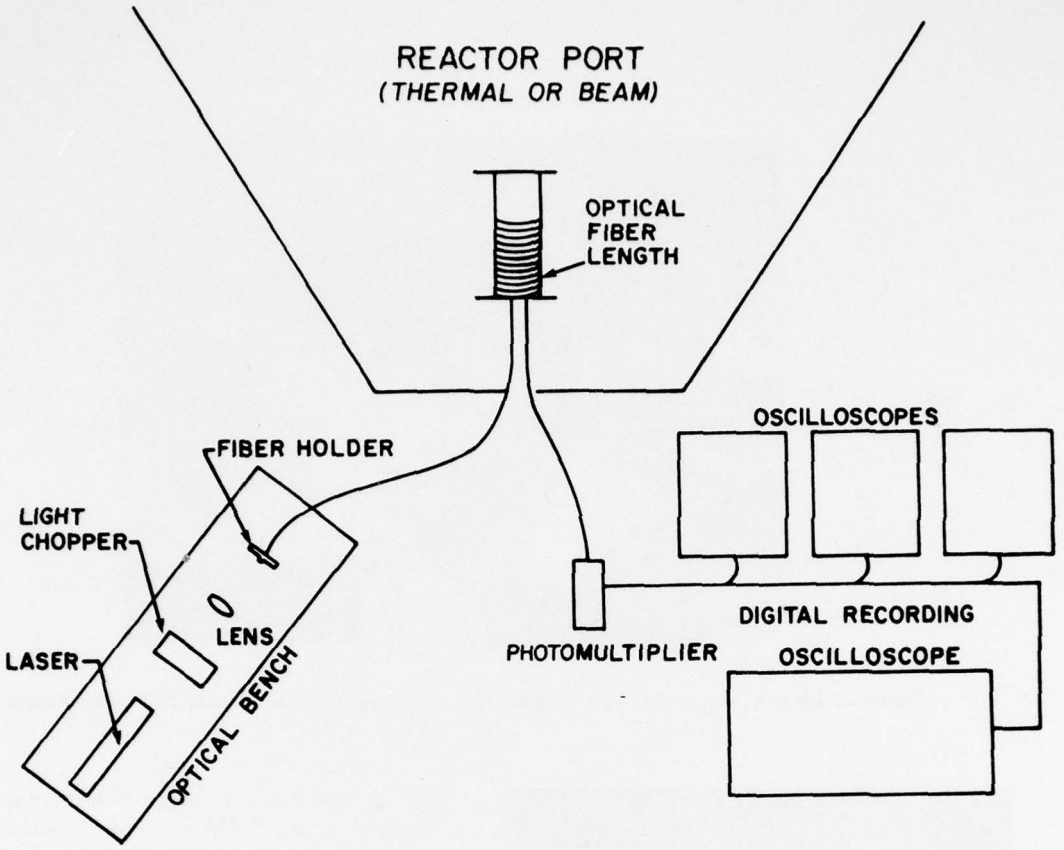

Figure 1. Basic experimental setup.

Focusing Lens

A lens was used to focus the laser beam onto the ends of fibers which have very small diameters. The lens, laser, and fiber-end holder were mounted on an optical bench to isolate them from any mechanical vibration. Figure 2 shows the illumination setup.

Optical Fiber Length

The optical fibers were wound around plexiglass cylinders, which were placed in one of the reactor ports. The length of each exposed fiber was accurately measured so that any attenuation change could be related to fiber length. Figure 3 shows a fiber wound on a cylinder, and Figure 4 shows a fiber entering the thermal port of the reactor. (See the appendix for a description of the reactor ports.)

Reactor Ports

The thermal and beam ports of the University of Illinois TRIGA Reactor* were used in this study.

*TRIGA (Training, Research, Isotope production, General Atomic) is a trademark of the General Atomic Division of the General Dynamics Corporation. The appendix describes the University of Illinois TRIGA reactor.

The thermal port was used in the first phase of the study because the energy of the neutrons in the port is primarily thermal (less than .025 eV). The total integrated thermal neutron flux at the position of the optical fiber in the thermal column was 10^{12} n/cm^2 per pulse, for a pulse level of 1900-MW peak. Since a total integrated flux level of 10^{12} n/cm^2 is the flux level possible at a distance of 1 mile (1.6 km) from the explosion of a 1-megaton device,[5] this flux level was considered acceptable for exposure of the optical fibers in the termal neutron effects phase of experimentation.

The beam port of the reactor was used in the second phase of the study. The optical fiber on the cylinder was placed in the beam port and the reactor was operated at a steady-state power level of 1.5 kW for 20 minutes. During this period, the total integrated fast neutron flux was 4×10^{11} n/cm^2, the total integrated thermal neutron flux was 4×10^{12} n/cm^2, and the gamma radiation dose was 2×10^4 roentgen; these levels were considered sufficient for the experiment.

[5]S. Glasstone, *The Effects of Nuclear Weapons* (United States Atomic Energy Commission, April 1962).

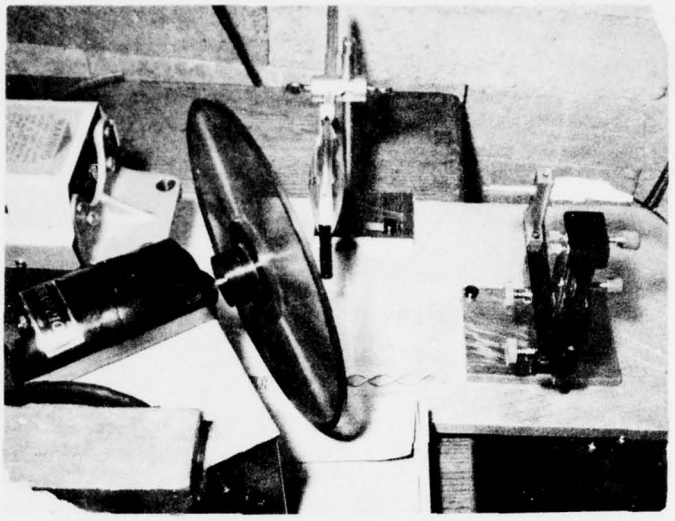

Figure 2. Illumination setup. Left to right: laser, chopper, focusing lens, and fiber-end holder.

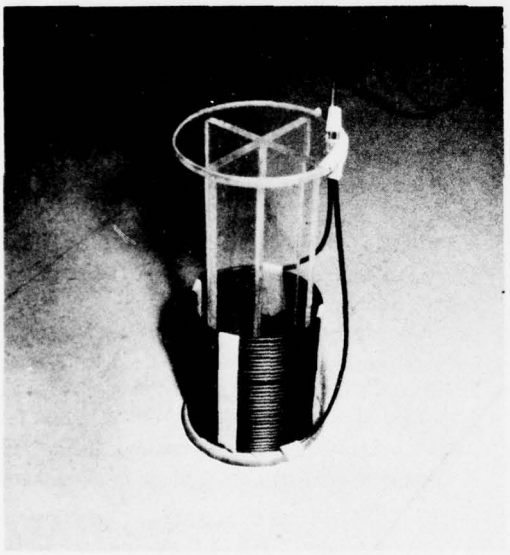

Figure 3. Optical fiber wound on cylinder.

Photomultiplier

A photomultiplier was used as a light level detector at the output end of the optical fiber. The photomultiplier used was constructed at CERL using a RCA-7102 photomultiplier tube. The 7102 has a S-1 spectral response having a spectral range of 4500 Å to 11500 Å; this response was compatible with the wave-length of the light source (6328 Å). The photomultiplier was used because of its high gain capability.

Oscilloscopes

Three oscilloscopes set at various time bases were used in the thermal neutron effects phase of the study to monitor the output of the photomultiplier during the reactor pulse. The oscilloscopes were triggered by a trigger pulse from the reactor control room at the instant the control rod was pulled out of the reactor to initiate a pulse. In addition, an uncompensated ion chamber (Westinghouse, Model #WL-6937) was used to compare the relative power levels of the individual pulses. The ion chamber's voltage output is proportional to the power output of the reactor.

Only one oscilloscope was used to monitor the output of the photomultiplier in the second phase of the study. Photographs of the scope trace were taken several times during the 20 minutes of steady-state radiation exposure.

Digital Recording Oscilloscope

In order to permit researchers to monitor the transmission of light through the optical fiber during and after the reactor pulse, a Macrodyne ERDAC III digital recording oscilloscope was used to digitize the output of the photomultiplier tube and record the digital data on magnetic tape. Each time period monitored was div-

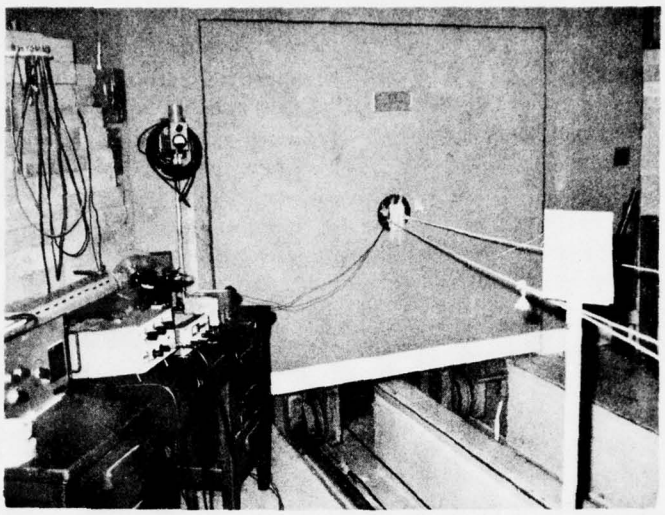

Figure 4. *Fiber entering thermal port.*

ided into 4096 samples, with the sampling interval set according to the length of the time period. Typical sampling intervals were from 0.2 msec to 0.5 msec. The amplitude of the signal can be resolved to one-thousandth of the full scale voltage range. Data collection using the ERDAC III made it possible to analyze the data using a minicomputer. The recording feature of the ERDAC III also provided an accurate record of the test data.

Radiation Dosage Monitoring

Determining the total neutron flux (thermal and fast) and gamma radiation dosage that the fibers were subjected to was necessary in both phases of the study. Three types of radiation detectors were used to obtain this information. Gold foils were used in conjunction with cadmium-covered gold foils to determine the total thermal neutron flux using the cadmium difference technique. Sulfur pellets were used in detecting fast neutrons (neutrons having energies greater than 3 MeV). Calcium fluoride thermoluminescent dosimeters (TLDs) were used in monitoring the gamma radiation dose. All the detectors were obtained from Edgerton, Germeshausen, and Grier, Inc., who provided a readout on the detectors after exposure.

Operational Procedures

Determination of Thermal Neutron Effects

The optical fibers wound around plexiglass cylinders were placed in the thermal port. Gold foil detectors were taped at both ends of the cylinders to obtain a measure of the average thermal neutron flux to which the fiber was subjected. A sulfur pellet and calcium fluoride TLD were placed on the first fiber sample to determine the fast neutron flux and gamma radiation dose present for a typical irradiation in the thermal port.

The light chopper was set so the laser beam was modulated into a square wave with a frequency of 215 Hz. The fiber end was aligned to obtain the peak amplitude signal from the photomultiplier.

The three oscilloscopes and digital recording oscilloscope were on a .285-second delay after the trigger pulse from the control room. The delay was needed to display the output signal of the photomultiplier just prior to the reactor pulse. The oscilloscope camera shutters were manually opened 2 seconds prior to the reactor pulse and closed after the reactor pulse. The digital recording oscilloscope was operated such that a 1-second interval of the photomultiplier output was

digitized and recorded various times after the reactor pulse. The samples were taken for 15 minutes after the pulse to measure the time duration and amplitude of radiation-induced attenuation. The samples were recorded on magnetic tape for subsequent analysis.

Prior to testing the fibers, the output of the photomultiplier (without light input) was monitored during a test pulse to determine whether radiation shielding was needed to protect the photomultiplier from any possible external radiation during the reactor pulse. The oscilloscope trace of the output signal showed that there was no effect on the photomultiplier, indicating that no shielding was needed.

Two of the three types of optical fibers were subjected to seven to ten reactor pulses, at 20- to 30-minute intervals. The medium-loss borosilicate fiber was only subjected to two reactor pulses; the fiber was completely opaque after the second pulse, making further testing impossible, since no light could be transmitted. The reactor was pulsed at a power level around 1900 MW; the actual power level of each pulse was recorded in the reactor control room.

Determination of Thermal Neutron, Fast Neutron, and Gamma Radiation Effects

The optical fibers were placed in the beam port of the reactor. The light chopper was set so the laser beam was modulated into a square wave with a frequency of 215 Hz. The end of the optical fiber was aligned to obtain the peak amplitude output signal from the photomultiplier.

To monitor the total neutron flux (fast and thermal), sulfur pellets and gold foils were placed on the fiber samples. Calcium fluoride TLDs were placed on the fibers to measure the accumulated gamma radiation dose.

The photomultiplier's output during its radiation exposure was monitored by taking both oscilloscope photographs and digital recording oscilloscope records. Oscilloscope pictures of the photomultiplier output were taken at various times during and after the radiation exposure. The digital recording oscilloscope was used to record 0.08-second intervals at various times during the radiation exposure.

Two types of optical fibers were used in this phase of experimentation: the low-loss, plastic-clad pure silica and all-plastic fibers. The fibers were subjected to a 20-minute radiation exposure with the reactor operating at a 1.5-kW steady-state power level.

3 DATA ANALYSIS

Attenuation Analysis

The amplitude of the square wave output of the photomultiplier at various times during and after the radiation exposure was measured to determine the duration and amplitude of radiation-induced attenuation changes in the optical fiber. The following sections discuss the techniques used in determining the amplitude of the square wave output for the two phases of the study and the method used to calculate the attenuation change.

Determination of Thermal Neutron Effects

The square wave amplitude was measured by examining the oscilloscope pictures taken during the reactor pulse and 0.5 seconds thereafter, and the record made by the digital recording oscilloscope during and up to 15 minutes after the pulse.

Although it was originally planned that the digital recording oscilloscope data would be analyzed by a minicomputer, the analyzing program was so sensitive to small variations in data that the computer could not be used. Instead, measurement of the square wave amplitude was accomplished by manually examining the recorded trace, using the cursor feature of the recording oscilloscope, which displays the amplitude of each recorded data point. Simple subtraction of the high and low states of the square wave will determine the amplitude. Several half cycles of the square wave were averaged to eliminate the effects of some 60-Hz noise present on the square wave output.

Determination of Fast Neutron Flux, Thermal Neutron Flux, and Gamma Radiation Effects

In this phase of the study, the amplitude of the square wave at various times during and after the irradiation was measured from oscilloscope pictures and recorded traces on the digital recording oscilloscope. Measurement of the square wave amplitude using the digital recording oscilloscope was done by averaging the high and low states of 20 square wave cycles at various times during and after the radiation exposure.

Calculation of Attenuation Change

The results of the square wave amplitude measurements were used to calculate the attenuation change, using Eq 1:

$$\Delta T = \frac{10 \log_{10} \frac{V}{V_o}}{L} \qquad \text{[Eq 1]}$$

where ΔT = change in attenuation dB/km

V_o = square wave amplitude prior to radiation exposure

V = square wave amplitude during or after radiation exposure

L = length of optical fiber exposed.

Luminescence Analysis

The output of the photomultiplier was monitored during the radiation exposure to determine the amplitude and time duration of luminescence. Luminescence was identified by a change in the output of the photomultiplier during both the off and on states of square wave. Figure 5 is an oscilloscope picture of the photomultiplier output during the reactor pulse; the downward change is due to luminescence.

The amplitude and time duration of the luminescence during the thermal neutron flux pulse was measured by the digital recording oscilloscope and analyzed by the minicomputer. The program used determined the magnitude of the downward change and its time duration. The luminescence present during the 1.5-kW steady-state exposure was too small for computer analysis, so the level of the off state of the square wave was manually determined using the cursor feature of the digital recording oscilloscope.

4 TEST RESULTS

Thermal Neutron Effects

Low-Loss Fused Silica Fibers

A 16.25-m length of low-loss fused silica fiber was used in this phase of the study. The length of the fiber placed in the thermal port of the reactor was 9.57 m. The fiber was subjected to ten reactor pulses with an average pulse level of 1800 MW.

Gold foils determined that the total accumulated thermal neutron flux for the ten pulses was 8.29×10^{12} n/cm^2, or an average thermal neutron flux of 8.29×10^{11} n/cm^2 per pulse. A sulfur pellet placed on the sample determined that the total accumulated fast neutron flux was 1.5×10^9 n/cm^2, or 1.5×10^8 n/cm^2 per pulse. The calcium fluoride TLD detected a dose of 3800 roentgen for the ten pulses, or 380 roentgen per pulse.

The low-loss fused silica fiber experienced a radiation-induced attenuation change which decayed rapidly from 14 dB/km to 6.3 dB/km in a period of 1.5 seconds after the reactor pulse. Figure 6 is a plot of the average attenuation change for six thermal neutron flux pulses. The attenuation change dropped from 6.3 dB/km to 0 dB/km in a time duration of 900 seconds; Figure 7 plots this decay. Thus, the low-loss fused silica

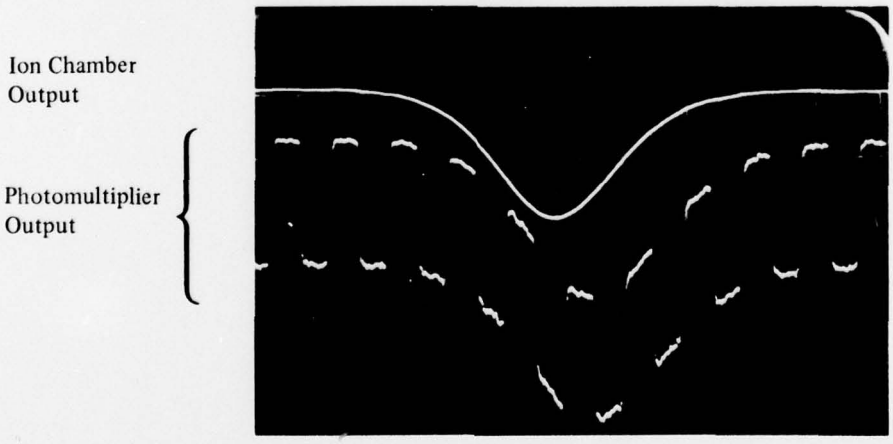

Figure 5. Square wave output of photomultiplier and ion chamber output during reactor pulse. Scale: 5 msec/division.

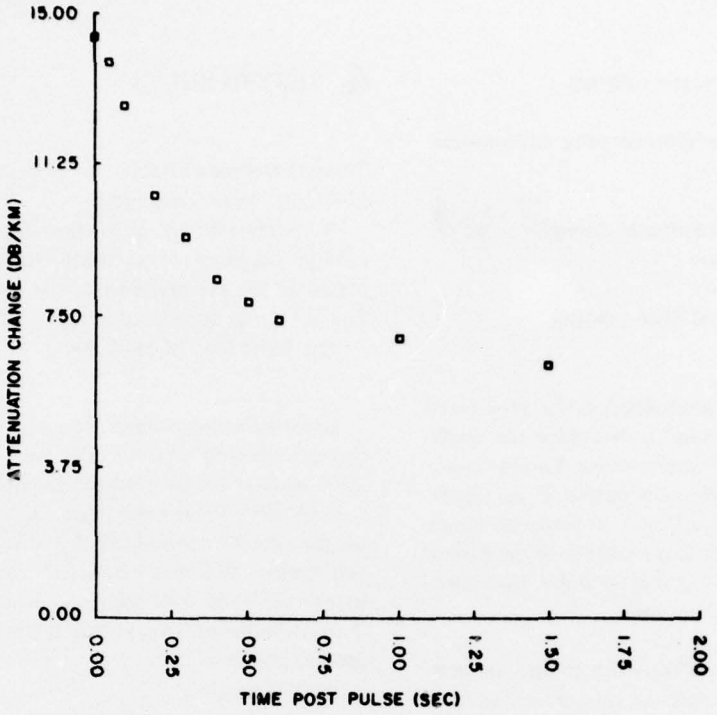

Figure 6. Low-loss fused silica fiber: average attenuation change vs time post pulse for six pulses.

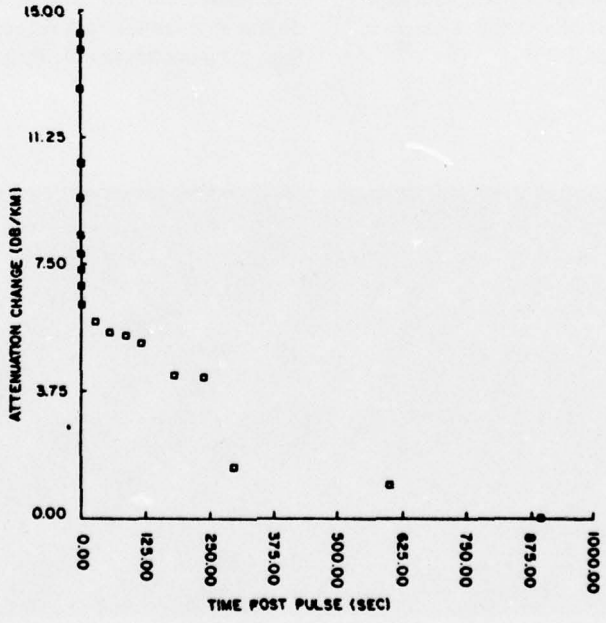

Figure 7. Low-loss fused silica fiber: decay of attenuation change.

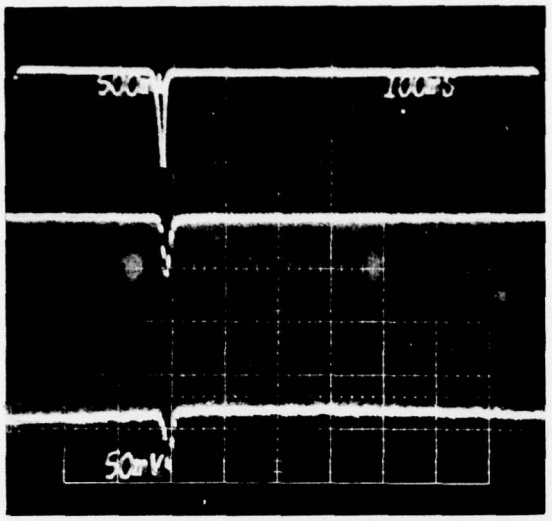

Figure 8. Luminescence in low-loss fused silica fiber during reactor pulse. Top trace is ion chamber output, which is proportional to the reactor output; bottom two traces are the top and bottom of the chopped square wave. Scale: 50 mV/vertical division; 100 msec/horizontal division.

fiber did not experience any permanent attenuation change. The fiber completely recovered within 900 seconds after each reactor pulse.

The short-term attenuation change was determined to be due to the thermal neutron flux. Fast neutron flux was eliminated as a possible cause based on results of a previous study by Wall and Bryant.[6] Their study indicated that the attenuation change induced by a fast neutron flux level equivalent to that present in this study is several orders of magnitude smaller than the attenuation change measured in this study.

The low-loss fused silica fiber did exhibit luminescence during the reactor pulse. The average amplitude of the luminescence for the ten reactor pulses was .05 V with a time duration of .02 seconds. Figure 8 is a scope picture of the luminescence of a fiber being subjected to a total integrated thermal neutron flux of 8×10^{11} n/cm^2.

[6]J. A. Wall and J. F. Bryant, *Radiation Effects on Fiber Optics*, AFCRL-TR-75-0190 (Air Force Cambridge Research Laboratories, 1975).

To determine the possible effect of the thermal neutron flux on a longer length of fiber, a 19.8-m length of the fiber was placed in the thermal port. The amplitude of the luminescence measured during the pulse was .17 V with a time duration of .02 seconds. The increased length of fiber subjected to the thermal neutron radiation allowed more energy to be absorbed by the optical fiber. The relationship between the increase in the length of the fiber and the corresponding increase in amplitude of luminescence was not determined in this study; the phenomenon was only identified.

Medium-Loss Borosilicate and Lead-Silicate Fiber

A 7.08-m length of fiber was placed in the thermal port of the reactor. After one reactor pulse with a total integrated thermal neutron flux of 7.62×10^{11} n/cm^2, the fiber experienced an attenuation change greater than 300 dB/km. Seventeen hours after the first pulse, the fiber recovered 50 dB/km, enough to allow a signal to be transmitted through it, and thus allow another pulse test.

After the second reactor pulse, no measurable signal could be transmitted through the fiber. Figure 9 shows an oscilloscope photograph of the transmitted square wave waveform, illustrating the sudden attenuation change.

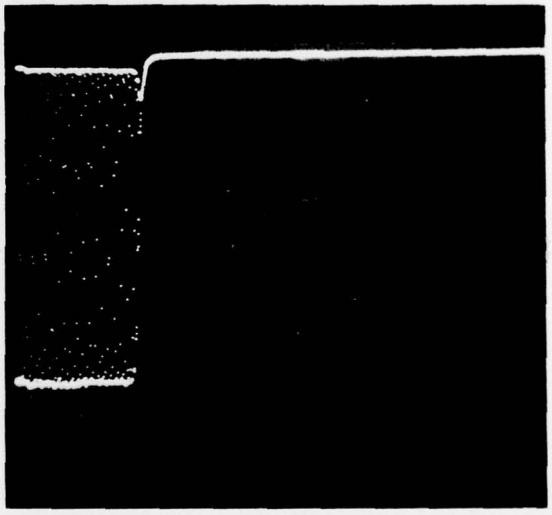

Figure 9. Massive attenuation change in medium-loss borosilicate fiber during first radiation exposure.

The massive permanent attenuation change in the fiber was probably due to the boron in the optical fiber material. Boron has a large cross section for absorbing neutrons, which results in changes in the optical transmission properties of the material. This fact makes optical fibers containing boron very susceptible to neutron radiation.

The fiber also exhibited luminescence during the reactor pulse. The amplitude of the luminescence was measured to be .03 V within a time duration of .022 seconds. During the second exposure, after the fiber had recovered slightly from the first exposure, the luminescence was measured to be 1 mV.

Plastic Fiber

A 14.97-m length of plastic monofilament fiber was used in the experiment; 7.66 m of the fiber were placed in the thermal port of the reactor and subjected to a total integrated thermal neutron flux level of 1×10^{12} n/cm^2 per pulse.

The plastic fiber had an initial increase in attenuation of about 10 dB/km just after the reactor pulse. The change in attenuation quickly began to recover to 0 dB/km within .3 seconds after the pulse. As the plot of the average attenuation change for seven reactor pulses (Figure 10) shows, the attenuation change started to become negative, meaning that the signal from the photomultiplier increased after the reactor pulse.

The increase in the output signal of the photomultiplier continued for several of the reactor pulses. Figure 11 plots the change in the pre-pulse square wave amplitude following seven reactor pulses. The net increase in the pre-pulse square wave amplitude was measured to be 2.23 dB for eight reactor pulses.

Four things could be causing this increase in the photomultiplier output:

1. An improvement in the photomultiplier's sensitivity
2. An increase in the laser beam's output
3. An improvement in the alignment of the laser beam and the end of the fiber
4. An actual improvement in the optical fiber's transmission properties.

Because the output signal of the photomultiplier improved over a 2-hour period, the probability of a component of the experimental setup causing this effect is small. An actual improvement in the optical fiber's transmission properties could be the reason for improvement. Radiation is known to change the hardness of plastic material; this change could in turn change the optical transmission properties of the plastic fiber material. Further investigation is needed to test this hypothesis.

The plastic fiber also exhibited luminescence during the reactor pulse. The average amplitude of the luminescence present was .245 V, with a time duration of .028 seconds. The amplitude of this luminescence was larger than that of the other two fibers, possibly because the plastic fiber did not have an outer jacket like the other fibers.

Fast Neutron Flux, Thermal Neutron Flux, and Gamma Radiation Effects

Plastic Fiber

A 13.5-m length of the plastic fiber was placed in the beam port of the reactor and subjected to a 20-minute exposure with accumulated thermal neutron flux of 5×10^{12} n/cm^2, an accumulated fast neutron flux of 5.86×10^{11} n/cm^2, and a gamma radiation dose of 2.5×10^4 roentgens.

During this exposure, the attenuation increased at a rate of 1.75 dB/km/minute. When the reactor was shut down, the fiber began to recover; recovery was complete 6 minutes after the power was shut down. The attenuation change then became negative; 20 minutes after the reactor was shut down the attenuation change was −15 dB/km/sec. Figure 12 is a plot of the attenuation change versus time.

This negative attenuation change is very similar to that of the plastic fiber in the thermal port. Again, the optical transmission properties of the fiber may have been improved due to the radiation exposure, but further investigation is necessary.

During the steady-state power level, a luminescence level of 4 mV (approximately 2 percent of the signal level) was measured from the output of the photomultiplier.

Low-Loss Fused Silica Fiber

A 10-79-m length of the low-loss fused silica fiber was also tested; 8.29 m of the overall length were placed in the beam port. The fiber was subjected to a 20-minute exposure with an accumulated thermal neutron flux of 3.87×10^{12} n/cm^2, an accumulated

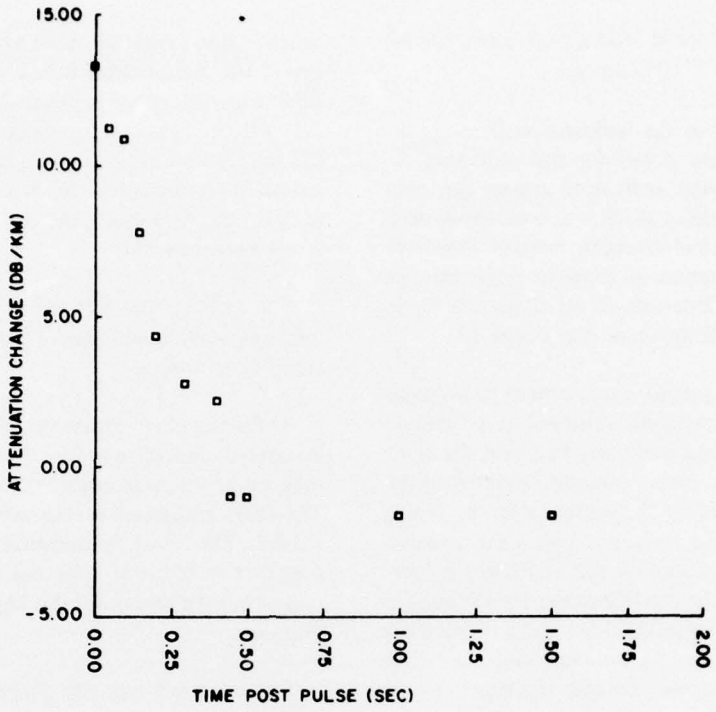

Figure 10. Plastic fiber: average attenuation vs time for seven reactor pulses.

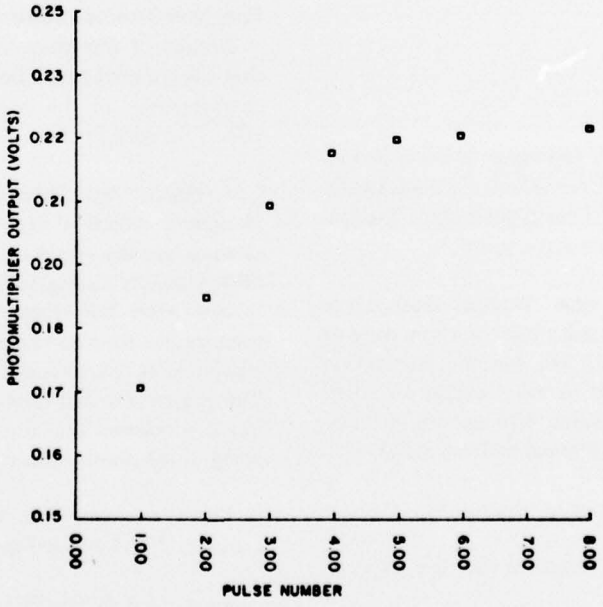

Figure 11. Plastic fiber: pre-pulse square wave amplitude following seven reactor pulses.

fast neutron flux of 3.64×10^{11} n/cm^2, and a gamma radiation dose of 2.19×10^4 roentgens.

Figure 13 is a plot of the indicated variation in the fiber attenuation. Data points for this plot were derived using minicomputer analysis to average the levels of the tops and bottoms of all 17 square waves recorded during each 0.082-second recording interval. This technique enabled a reduction in apparent noise through long-term averaging. Intervals of recording are represented by the timing of data points in Figure 13.

The data indicate a slight improvement in transmission within the first 2 seconds, followed by a 7-minute period when light transmission was less than the starting value. During the first 5 minutes, attenuation increased 15 dB/km. From 5 minutes after beginning exposure to 25 minutes after, however, light transmission improved. The reasons for this improvement were not determined, but the possible causes are the same as for the plastic fiber. Since this fiber has a plastic cladding, radiation hardening of the material is a possible cause of the improvement. Further investigations are necessary to analyze these effects.

The luminescence level during this exposure was too small to measure.

5 CONCLUSIONS

Thermal Neutron Effects

Results of this phase of experimentation indicated that thermal neutron flux does affect the transmission characteristics of the three fiber types tested. The specific effects for each fiber are given below.

1. Low-loss fused silica fiber. Thermal neutron flux levels of 10^{12} n/cm^2 induced a temporary increase in attenuation of about 14 dB/km, but the attenuation decayed rapidly to one-half its value within 1 second. The fiber fully recovered within 900 seconds (15 minutes) after exposure to the thermal neutron radiation.

Luminescence was detected during the thermal neutron flux exposure. The amplitude of the luminescence increased when the length of the fiber exposed was increased.

2. Medium-loss borosilicate and lead-silicate fiber. This fiber was found to be very susceptible to thermal neutron flux exposure. After exposure to a total integrated thermal neutron flux level of 10^{12} n/cm^2, the fiber experienced an increase in attenuation of over 300 dB/km. The change in attenuation was for all practical purposes permanent. Because of the massive, permanent attenuation increase, use of this type of optical fiber in possible thermal neutron environments is not recommended.

The medium-loss borosilicate and lead-silicate fiber also exhibited luminescence during the thermal neutron flux exposure.

3. Plastic fiber. Exposure of this fiber to a total integrated thermal neutron flux level of 10^{12} n/cm^2 induced an initial increase in attenuation of 10 dB/km. The fiber recovered to the original state within 0.3 seconds. The fiber's transmission characteristics actually appeared to improve after exposure to several reactor pulses, but the reason for this improvement was not determined.

Luminescence was also present during the thermal neutron exposure. The amplitude of this luminescence was larger than the luminescence present during irradiation of the other fibers, possibly because the plastic fiber did not have an outer jacket like the other fibers.

Fast Neutron Flux, Thermal Neutron Flux, and Gamma Radiation Effects

Results of this phase of experimentation indicated that the combined radiation did affect the transmission characteristics of the two fibers tested. The specific effects for each fiber are given below.

1. Plastic fiber. Subjection of the plastic fiber to a 20-minute radiation exposure induced an increase in attenuation; the attenuation increased at a rate of 1.75 dB/km/minute during the exposure. The fiber began to recover after the reactor was shut down; within 6 minutes, the fiber had completely recovered. The fiber's transmission characteristics then appeared to improve. The reason for this improvement was not identified, but it is believed that it may be due to radiation hardening of the plastic optical material.

During the combined radiation exposure, a luminescence level of 4 mV was measured in the plastic fiber.

2. Low-loss fused silica fiber. During the first 5 minutes of the 20-minute exposure in the combined radiation environment, the low-loss fused silica fiber exhibited an increase in attenuation of 15 dB/km. The fiber

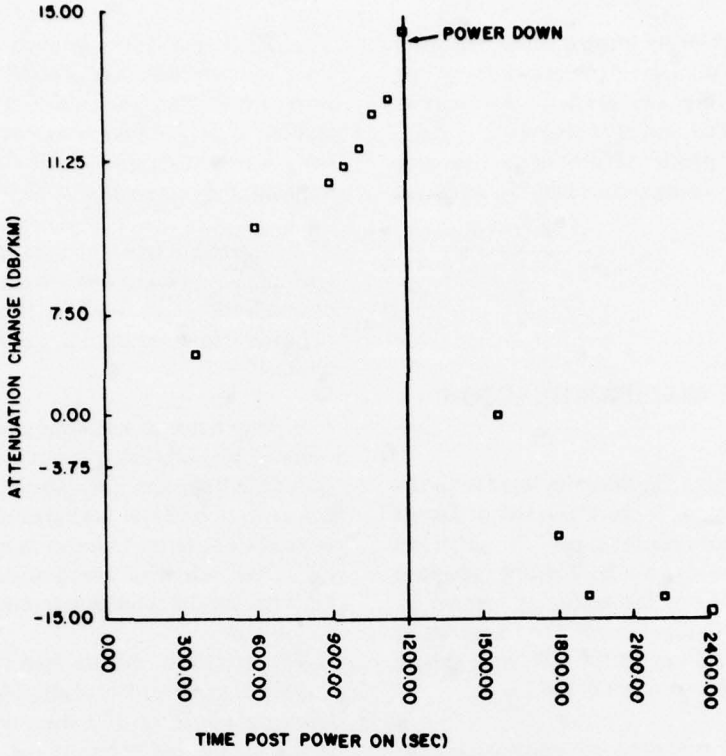

Figure 12. Plastic fiber attenuation change vs time during and after 1.5 kW operation.

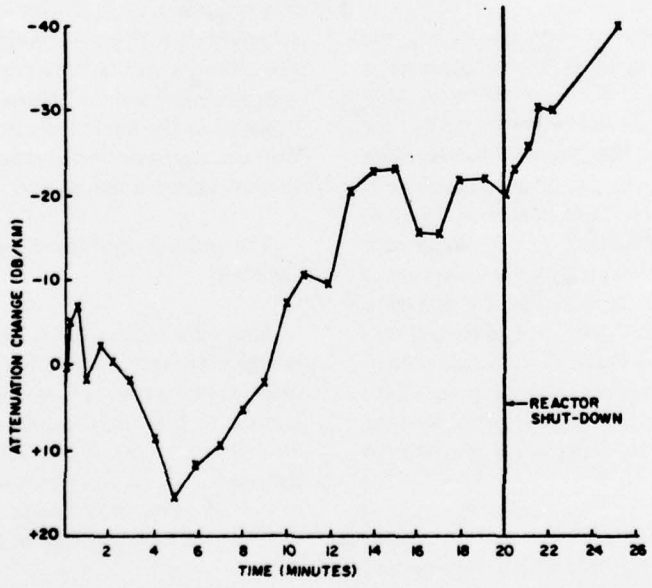

Figure 13. Attenuation change of low-loss fiber in beam port.

then began to recover to its original condition. After recovery, the light transmission characteristics of the fiber appeared to improve. The reason for this improvement was not identified, but it is believed that radiation hardening of the plastic cladding of the fiber may be the cause. No luminescence could be measured during the exposure.

APPENDIX: DESCRIPTION OF NUCLEAR REACTOR

The nuclear reactor used in this study was the Illinois Advanced TRIGA Reactor at the University of Illinois at Urbana-Champaign. Primarily a research reactor designed to furnish neutrons (or other ionizing radiation) for experimental purposes, the reactor is licensed by the U. S. Nuclear Regulatory Commission to operate at steady-state power levels up to 1.5 MW, with pulsing capabilities to a peak power of 6000 MW.

The pulsed type of operation is possible because of an inherent safety characteristic of the reactor fuel (a hydrided uranium-zirconium alloy), which has a large prompt negative fuel temperature coefficient. As the fuel temperature increases, the prompt negative fuel temperature coefficient acts as a shutdown mechanism.

Following a step insertion of positive reactivity, the reactor power increases until a fuel temperature is reached at which the loss of reactivity due to the negative temperature coefficient will compensate for the reactivity inserted. As the fuel temperature continues to rise beyond this point, there is an increasing loss of reactivity with a subsequent power decrease. In other words, the power increase is terminated by the prompt negative temperature coefficient. With the exception of the reactor period, which depends on the reactivity inserted, the parameters of a pulse depend on the feedback effects of the prompt negative temperature coefficient. Thus, the time to peak and the pulse width depend on the magnitude of the pulse, with the time to peak being shorter and the pulse width narrower for larger pulses.

The reactor power level is determined by several control rods (graphite-impregnated with boron carbide) which contain a poison (boron) to absorb neutrons. The reactor has five control rods:

1. Three manually operated control rods. These three rods are manually controlled by motors located above the reactor. They also contain a fuel-moderator section below the poison section to increase the reactivity worth of the rod and give a uniform flux distribution in the core when the rod is withdrawn.

2. Adjustable transient rod. This rod, which can be operated pneumatically as well as manually, has a poison section with an air follower. The stroke length of the rod can be adjusted according to the size of the desired transient.

3. Fast transient rod. This control rod can only be operated pneumatically. It has an air follower like the adjustable transient rod, but it has a double-length poison section so that the initial acceleration of the rod takes place without a change in reactivity. As a result, the actual reactivity insertion occurs at a faster rate than that for the adjustable transient rod.

The latter two rods are used for pulsed operations. The reactivity insertion of the adjustable transient rod takes place in about 100 msec, while the reactivity insertion of the fast transient rod takes place in about 50 msec. When both rods are used, a delay circuit is employed so that the ends of the reactivity insertions occur at the same time.

To initiate a pulse, the reactor is brought to critical at a low power (e.g., 15 W) using the manually driven control rods with both transient rods in the down position. When a critical condition is reached, the transient rods are armed and the adjustable transient rod cylinder is placed in the desired position. The transient rods are then pneumatically withdrawn resulting in a step insertion of positive activity.

The pulse is monitored by an uncompensated ion chamber.

Since the reactor is designed for experimental purposes, a number of experimental facilities have been included in the design of the reactor. Of particular interest to this study are the thermal column and the through beam port. Figure A1 shows a cross section of the reactor at the beam port level. The detail of the location of other beam ports and other experimental facilities has been omitted in the figure for simplicity.

The thermal column is a section of moderator (graphite) which extends from the outer face of the reflector,

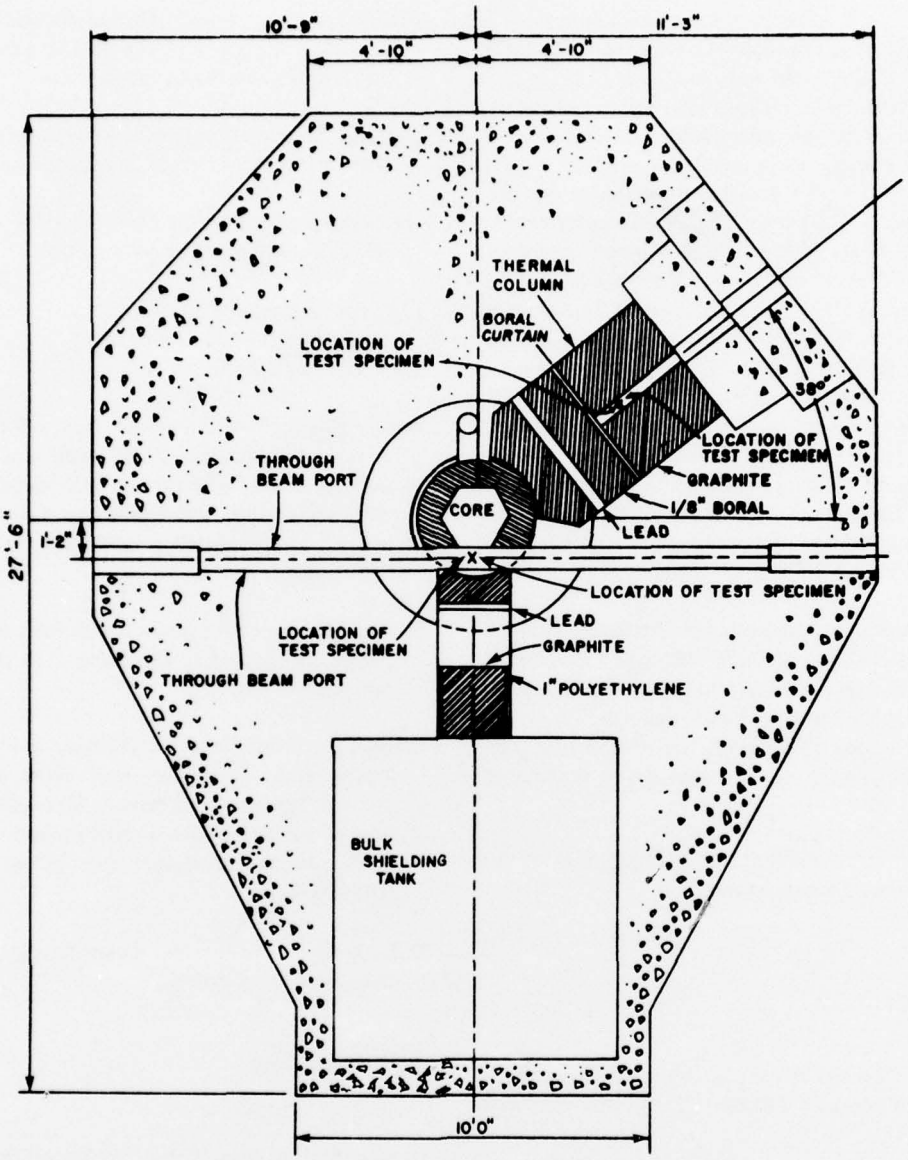

Figure A1. Section at port level showing location of thermal column and through beam port. SI conversion factors: 1 ft = 0.3048 m; 1 in. = 25.4 mm.

which surrounds the reactor core, through the reactor pool and concrete shield to a high density concrete door, which is mounted on tracks and may be removed. The graphite section (4 ft × 4 ft × 5.5 ft in length [1.2 m × 1.2 m × 1.7 m]) is surrounded by a welded aluminum container fabricated from 1/2-in. (12.7 mm) thick sheets of aluminum and lined with 1/2-in. (12.7 mm) thick boral (boron-aluminum) sheets to reduce capture gammas in the surrounding concrete. To reduce the gamma ray background, a 4-in. (101.6 mm) thick lead shield is placed within the graphite approximately 50 in. (1.3 m) from the outside surface (near the concrete door) of the thermal column. Approximately 3 ft (0.9 m) from the outside surface is a 1/4-in. (6.3 mm) thick boral sheet which may be raised or lowered to control the slow neutron flux in the outer region of the graphite section. Nine of the 4-in. × 4-in. × 36-in. (101.6 mm × 101.6 mm × 0.9 m) graphite blocks in the outer section of the thermal column may be removed for experimental work. During this study, one of the graphite blocks was removed, the boral curtain raised, and the concrete door closed. The optical fiber was situated approximately 2 ft (0.6 m) from the outer surface of the thermal column.

The through beam port extends completely through the reactor shield and the core reflector. This permits placement of a test specimen in a region adjacent to the reactor core to obtain a higher neutron flux. In the experiments in the beam port, the optical fiber was placed in a position as nearly tangential to the core as possible.

Beck[7] provides a more complete description of the Illinois Advanced TRIGA Reactor.

GLOSSARY

attenuation: The loss in propagating light power in optical fibers normally expressed per unit of length in decibels as

$$\text{Attenuation} = 10 \log P_1 / P_2$$

where P_1 = power propagating at the reference point of interest.

P_2 = power propagating after passing through a unit fiber length.

attenuation (short term): That attenuation (increase) which occurs after subjection of a fiber to a radiation dose but which lasts less than 1 minute.

attenuation (long term): That attenuation which occurs after subjection of the fiber to a radiation dose which lasts more than 1 minute.

cladding: The outer portion of an optical fiber having a different index of refraction than the core.

core: The center portion of a step-index optical fiber having a constant index of refraction.

EMI: electromagnetic interference.

EMP: electromagnetic pulse.

fast neutrons: Neutrons which have velocities corresponding to a band of energy levels; this band is normally defined as from 10 keV to 20 MeV. For purposes of this report, however, fast neutrons are defined as those with greater energy than thermal neutrons.

jacket: The protective outer sheath (usually a form of plastic) of an optical fiber cable. The jacket has no optical function.

thermal neutrons: Neutrons which are in thermal equilibrium with a medium near room temperature (20°C). The neutrons have a Maxwellian distribution of velocities with a most probable velocity of 2200 m/second (corresponding to an energy of 0.6253 eV).

TLD: A thermoluminescent dosimeter used to measure gamma radiation dosage.

REFERENCES

Beck, G. P. et al., *Safety Analysis Report for the Illinois Advanced TRIGA* (University of Illinois, January 1971).

Gallawa, R. L., *Optical Fiber Links for Telecommunication* (U. S. Army Strategic Communications Command, 1973).

Glasstone, S., *The Effects of Nuclear Weapons* (United States Atomic Energy Commission, April 1962).

[7] G. P. Beck et al., *Safety Analysis Report for the Illinois Advanced TRIGA* (University of Illinois, January 1971).

Manual, R. D., E. J. Shiel, S. Kronenburg, and R. A. Lux, "Effect of Neutron- and Gamma Radiation on Glass Optical Waveguides," *Applied Optics* (September 1973).

Mattern, P. L., L. M. Watkins, C. D. Skoog, J. R. Brandon, and E. H. Barsis, *The Effects of Radiation on the Absorption and Luminescence of Fiber Optic Waveguides and Materials* (Sandia Laboratories, 1974).

McCormack, R. G. and D. C. Sieber, *Fiber Optic Communications Link Performance in EMP and Intense Light Transient Environments*, Interim Report E-94/ADA032126 (U. S. Army Construction Engineering Research Laboratory, 1976).

Wall, J. A. and J. F. Bryant, *Radiation Effects on Fiber Optics*, AFCRL-TR-75-0190 (Air Force Cambridge Research Laboratories, 1975).

CERL DISTRIBUTION

US Army, Europe
ATTN: AEAEN

Director of Facilities Engineering
APO New York 09827

DARCOM STIT-EUR
APO New York 09710

USA Liaison Detachment
ATTN: Library
New York, NY 10007

West Point, NY 10996
ATTN: Dept of Mechanics
ATTN: Library

Chief of Engineers
ATTN: Tech Monitor
ATTN: DAEN-ASI-L (2)
ATTN: DAEN-FEP
ATTN: DAEN-FEU
ATTN: DAEN-FEZ-A
ATTN: DAEN-MCZ-S
ATTN: DAEN-RDL

ATTN: DAEN-PMS (7)
for forwarding to
National Defense Headquarters
Director General of Construction
Ottawa, Ontario K1A0K2
Canada

Canadian Forces Liaison Officer (4)
US Army Mobility Equipment
Research and Development Command
Ft Belvoir, VA 22060

Division of Bldg Research
National Research Council
Montreal Road
Ottawa, Ontario, K1A0R6

Airports and Const. Services Dir.
Technical Information Reference
Centre
K40L, Transport Canada Building
Place de Ville
Ottawa, Ontario, Canada, K1A0N8

Aberdeen Proving Ground, MD 21005
ATTN: AMXHE/J. D. Weisz

Ft Belvoir, VA 22060
ATTN: ATSE-TD-TL (2)
ATTN: Kingman Bldg, Library

Ft Monroe, VA 23651
ATTN: ATEN
ATTN: ATEN-FE-U

Ft Lee, VA 23801
ATTN: DRXMC-D (2)

Ft McPherson, GA 30330
ATTN: AFEN-FEB

US Army Foreign Science & Tech Center
ATTN: Charlottesville, VA 22901
ATTN: Far East Office

USA-WES
ATTN: Library

6th US Army
ATTN: AFKC-LG-E

US Army Engineer District
Saudi Arabia
ATTN: Library
Pittsburgh
ATTN: Library
ATTN: Chief, Engr Div
Philadelphia
ATTN: Library
ATTN: Chief, NAPEN-D

US Army Engineer District
Norfolk
ATTN: Chief, NAOEN-M
Huntington
ATTN: Library
ATTN: Chief, ORHED-D
Wilmington
ATTN: Chief, SAWEN-D
Charleston
ATTN: Chief, Engr Div
Savannah
ATTN: Library
ATTN: Chief, SASAS-L
Mobile
ATTN: Chief, SAMEN-C
Nashville
ATTN: Library
Memphis
ATTN: Library
ATTN: Chief, LMMED-DM
Vicksburg
ATTN: Chief, Engr Div
Louisville
ATTN: Chief, Engr Div
Detroit
ATTN: Library
St Paul
ATTN: Chief, ED-D
Rock Island
ATTN: Library
ATTN: Chief, Engr Div
St Louis
ATTN: Library
ATTN: Chief, ED-D
Kansas City
ATTN: Library (2)
ATTN: Chief, Engr Div
Omaha
ATTN: Chief, Engr Div
New Orleans
ATTN: Library
ATTN: Chief, LMNED-DG
Little Rock
ATTN: Chief, Engr Div
Fort Worth
ATTN: Chief, SWFED-D
Galveston
ATTN: Chief, SWGAS-L
ATTN: Chief, SWGED-DM
Albuquerque
ATTN: Library
San Francisco
ATTN: Chief, Engr Div
Sacramento
ATTN: Chief, SPKED-D
ATTN: Library, Room 8307
Far East
ATTN: Chief, Engr Div
Japan
ATTN: Library
Portland
ATTN: Chief, DB-3
Seattle
ATTN: Chief, EN-DB-EM
ATTN: Chief, NPSEN-PL-WC
Walla Walla
ATTN: Library
ATTN: Chief, Engr Div
Alaska
ATTN: Library
ATTN: Chief, NPADE-R

US Army Engineer Division
Europe
ATTN: Technical Library
New England
ATTN: Chief, NEDED-T
North Atlantic
ATTN: Chief, NADEN-T
Middle East (Rear)
ATTN: MEDED-T
South Atlantic
ATTN: Chief, SADEN-TE/TM
ATTN: Library

US Army Engineer Division
Huntsville
ATTN: Library (2)
ATTN: Chief, HNDED-ME
ATTN: Chief, HNDED-SR
Lower Mississippi Valley
ATTN: Library
Ohio River
ATTN: Library
ATTN: Chief, Engr Div
North Central
ATTN: Library
Missouri River
ATTN: Library (2)
ATTN: Chief, MRDED-T
Southwestern
ATTN: Library
ATTN: Chief, SWDED-TM
Pacific Ocean
ATTN: Chief, Engr Div
North Pacific
ATTN: Chief, Engr Div

Facilities Engineers
Carlisle Barracks, PA 17013
Ft Campbell, KY 42223
FORSCOM
Ft Devens, MA 01433
USAECOM
Ft Monmouth, NJ 07703
DSCPER
West Point, NY 10996
USATCFE
Ft Eustis, VA 23604
USAIC
Ft Benning, GA 31905
USAAVNC
Ft Rucker, AL 36361
CAC&FL (3)
Ft Leavenworth, KS 66027
USACC
Ft Huachuca, AZ 85613
TRADOC
Ft Monroe, VA 23651
Ft Gordon, GA 30905
Ft McClellan, AL 36201
Ft Sill, OK 73503
Ft Bliss, TX 79916
HQ, 7th Inf Div & Ft Ord, CA 93941
HQ, 24th Inf & Ft Stewart, GA 31313
HQ, 1st Inf Div & Ft Riley, KS 66442

AF/PREEU
Bolling AFB, DC 20332

AF Civil Engr Center/XRL
Tyndall AFB, FL 32401

Little Rock AFB
ATTN: 312/DEEE (Mr. Gillham)

Naval Air Systems Command
ATTN: Library
WASH DC 20360

Port Hueneme, CA 93043
ATTN: Library (Code L08A)
ATTN: Moreell Library

Washington DC
ATTN: Building Research Advisory Board
ATTN: Library of Congress (2)
ATTN: Dept of Transportation Library

Defense Documenation Center (12)

Engineering Societies Library
New York, NY 10017

Commander
Naval Facilities Engineering Command
ATTN: Code 04
200 Stovall St
Alexandria, VA 22332

Commander
Naval Undersea Center
ATTN: Code 6511, McCardell
San Diego, CA 92132

Commander
USACEEIA
ATTN: CCC-S
Ft Huachuca, AZ 85613

U.S. Army Electronics Command
ATTN: ANSEL-NL-RM-1
Ft Monmouth, NJ 07703

Naval Electronics Laboratory Center
271 Catalina Blvd
San Diego, CA 92152

Naval Avionic Facility
ATTN: Dept 844
6000 E. 21st St
Indianapolis, IN 46218

Headquarters
Defense Nuclear Agency
Technical Library
WASH DC 20315